sponding to region 6 in Fig. 6. Both pathways appear to be feasible. Supposedly, the second combined compression/twist pathway is preferentially proceeded by complexes with two chelate ligands, whereas the previous pure compression pathway is followed by complexes without steric constraints due to chelation. In addition, any preference (or combination of both) presumably depends on the electronic properties of the metal atom.

As already found in the study of spiro-carbon (Luef *et al.*, 1987), no strong correlation among bond-length deformations seems to be present.

References

ALLEN, F. A., BELLARD, S., BRICE, M. D., CARTWRIGHT, B. A., DOUBLEDAY, A., HIGGS, H., HUMMELINK, T., HUMMELINK-PETERS, B. G., KENNARD, O., MOTHERWELL, W. D. S., RODGERS, J. R. & WATSON, D. G. (1979). *Acta Cryst.* B35, 2331–2339.
ALLEN, F. H., KENNARD, O. & TAYLOR, R. (1983). *Acc. Chem. Res.* 16, 146–153.
ANDERSON, D. N. & WILLETT, R. D. (1974). *Inorg. Chim. Acta*, 8, 167–175.
AUF DER HEYDE, T. P. E., BUDA, A. B. & MISLOW, K. (1991). *J. Math. Chem.* 6, 255–265.
AUF DER HEYDE, T. P. E. & BÜRGI, H. B. (1989). *Inorg. Chem.* 28, 3960–3989.
BEATTIE, J. K. (1988). *Adv. Inorg. Chem.* 32, 1–53.
BOERE, R. T., MONTGOMERY, C. D., PAYNE, N. C. & WILLIS, C. J. (1985). *Inorg. Chem.* 24, 3680–3687.
BRITTON, D. & DUNITZ, J. D. (1981). *J. Am. Chem. Soc.* 103, 2971–2979.
BUDA, A. B., AUF DER HEYDE, T. & MISLOW, K. (1992). *Angew. Chem.* 104, 1012–1031; *Int. Ed. Engl.* 31, 989–1007.
BÜRGI, H. B. (1973). *Inorg. Chem.* 12, 2321–2325.
BÜRGI, H. B. & DUNITZ, J. D. (1983). *Acc. Chem. Res.* 16, 153–161.
BÜRGI, H. B., DUNITZ, J. D. & SHEFTER, E. (1973). *J. Am. Chem. Soc.* 95, 5065–5067.
BYE, E., SCHWEIZER, W. B. & DUNITZ, J. D. (1982). *J. Am. Chem. Soc.* 104, 5893–5898.
CHANDRASEKAR, K. & BÜRGI, H. B. (1983). *J. Am. Chem. Soc.* 105, 7081–7093.
DUNITZ, J. D. (1979). *X-ray Analysis & Structure of Organic Molecules.* New York: Cornell Univ. Press.
FACKLER, J. P. JR & MASTERS, A. F. (1980). *Inorg. Chim. Acta*, 39, 111–118.
FERRARO, J. R. & LONG, G. J. (1975). *Acc. Chem. Res.* 8, 171–178.
GERDAU, T. & KRAMOLOWSKY, R. (1982). *Z. Naturforsch. Teil B*, 37, 332–340.
HAHN, M. & WIPKE, W. T. (1988). *Tetrahed. Comput. Method.* 1, 81–86.
HAYTER, R. G. & HUMIEC, F. S. (1965). *Inorg. Chem.* 4, 1701–1706.
KILBOURN, B. T. & POWELL, H. M. (1970). *J. Chem. Soc.* pp. 1688–1693.
KLEBE, G. (1985). *J. Organomet. Chem.* 293, 147–159.
KLEBE, G. (1987). *J. Organomet. Chem.* 332, 35–46.
KLEBE, G. (1990). *Struct. Chem.* 1, 597–616.
KAFTORY, M., NUGIEL, D. A., BIALI, S. E. & RAPPOPORT, Z. (1989). *J. Am. Chem. Soc.* 111, 8181–8191.
LA MAR, G. N. & SHERMAN, E. O. (1969). *J. Am. Chem. Soc.* 92, 2691–2699.
LUEF, W. & KEESE, R. (1992). *J. Mol. Struct. Theochem.* 257, 353–368.
LUEF, W., KEESE, R. & BÜRGI, H. B. (1987). *Helv. Chim. Acta*, 70, 534–542.
MURRAY-RUST, P., BÜRGI, H. B. & DUNITZ, J. D. (1979). *Acta Cryst.* A35, 703–714.
NØRSKOV-LAURITZEN, L. & BÜRGI, H. B. (1985). *J. Comput. Chem.* 6, 216–228.
SHELDRICK, G. M. (1988). *XP-Plot Program.* Univ. of Göttingen, Germany.
TRIPOS ASSOCIATES (1991). *SYBYL.* Tripos Associates, St Louis, MO 63144, USA.

Structure of Sodium Ammonium (+)-Tartrate Tetrahydrate at 200, 151 and 120 K

BY Z. BROŻEK AND K. STADNICKA

Faculty of Chemistry, Jagiellonian University, ul. Ingardena 3, 30-060 Kraków, Poland

Abstract

The crystal structure investigation of $NaNH_4(+)$-$C_4H_4O_6.4H_2O$, known also as NAT, SAT or ARS (ammonium Rochelle salt), was carried out in order to determine the absolute chirality and to trace possible structural changes in the paraelectric phase from room temperature down to the region close to the ferroelectric phase transition at about 110 K. The observed relative elongation of the thermal ellipsoids in the [100] direction and hydrogen-bonding reorganization near the temperature 150 K support the idea of either a long-range preparation to the ferroelectric phase transition or an additional structure reconstruction, possibly without symmetry changes, at about 150 K. Additionally, the structure

at room temperature has been discussed from the point of view of the intermolecular atomic arrangements responsible for the sign of the gyration tensor components. Crystal data: $NaNH_4[(2R,3R)-C_4H_4O_6].4H_2O$, $M_r = 261.16$, orthorhombic, $P2_12_12$, $Z = 4$, $\lambda(Cu\ K\alpha) = 1.54178$ Å. At 200 K, $a = 12.112\ (1)$, $b = 14.310\ (17)$, $c = 6.204\ (1)$ Å, $V = 1075\ (1)$ Å^3, $D_x = 1.613$ g cm^{-3}, $\mu = 17.11$ cm^{-1}, $R = 0.0344$ for 1220 observed unique reflections. At 151 K, $a = 12.088\ (2)$, $b = 14.281\ (31)$, $c = 6.192\ (1)$ Å, $V = 1069\ (2)$ Å^3, $D_x = 1.623$ g cm^{-3}, $\mu = 17.22$ cm^{-1}, $R = 0.0334$ for 1221 observed unique reflections. At 120 K, $a = 12.065\ (6)$, $b = 14.346\ (7)$, $c = 6.165\ (3)$ Å, $V = 1067\ (1)$ Å^3, $D_x = 1.626$ g cm^{-3}, $\mu = 17.20$ cm^{-1}, $R = 0.0376$ for 1216 observed unique reflections.

Introduction

Crystals of sodium ammonium tartrate tetrahydrate, NAT, were the first to be separated successfully by L. Pasteur as left- and right-handed optical enantiomers (Lowry, 1964). The structure of NAT is isomorphous (Beevers & Hughes, 1941) with Rochelle salt (RS), $NaKC_4H_4O_6.4H_2O$, which was the first ferroelectric material discovered (Jona & Shirane, 1962). NAT crystals show interesting physical properties, not only near the first-order ferroelectric phase transition at about 110 K (which has attracted the attention of many scientists, see Table 1), but also in the paraelectric phase. There are several theoretical concepts concerning a possible mechanism of the ferroelectric phase transition (Aizu, 1971, 1984, 1986a,b, 1990; Sawada & Takagi, 1972; Ishibashi & Takagi, 1975; Sannikov & Levanyuk, 1977) but none of them is supported by a reliable structure determination of either the ferroelectric phase or the paraelectric phase in its low-temperature region. For the ferroelectric phase only preliminary X-ray data have so far been published (Sawada & Takagi, 1971; Iizumi & Gesi, 1978) whereas the structure determination of the paraelectric phase has been performed only at room temperature, RT (Beevers & Hughes, 1941; Shkuratova, Kiosse & Malinovskii, 1979; Kuroda & Mason, 1981).

The paraelectric phase reveals interesting optical properties. In particular, it shows a strong temperature and wavelength dependence of the angle between the optic axes, $2V$, which passing its zero value at a certain wavelength and temperature, e.g. $\lambda = 632.8$ nm and $T = 151$ K, leads to a pseudo-uniaxial state (Gaba, Kostetskii & Romanyuk, 1980). Spectral-temperature diagrams (Romanyuk, Gaba & Kostetskii, 1981; Gaba, Zheludev, Kostetskii & Romanyuk, 1983) are divided into three biaxial regions by curves representing the pseudo-

uniaxial states, one in the ferroelectric and the other in the paraelectic phase. In region I the plane of optic axes corresponds to the crystallographic plane ab, (001), in region II to ac, (010), and in region III to bc, (100). The pseudo-uniaxial state separating regions II and III extends over a wide range of wavelengths (including infrared and a part of the visible range) within the nearest vicinity of 150 K.

The variation of the $2V$ angle is followed by changes in the sign and magnitude of the optical rotatory power (ORP) measured along one of the symmetry-related optic axes, both with wavelength and temperature (Koralewski & Szafrański, 1988). This indicates a different contribution of the gyration tensor components to the value of ORP along the optic axis, depending on the position of the optic axes plane and the value of the $2V$ angle. The reported dispersion of ORP with temperature at $\lambda = 632.8$ nm clearly shows the optical uniaxial state at about 151 K.

Curves describing the temperature dependence of the birefringence for NAT crystals, especially $\Delta n_y = n_x - n_z$ and $\Delta n_z = n_x - n_y$ also exhibit (for $\lambda = 700$ nm) a significant change of slope at about 150 K which is not obviously related to the corresponding dilatation coefficients presented in the same publication (Romanyuk, Gaba & Kostetskii, 1981). Moreover, the linear thermal expansion coefficients, α_x and α_y, versus temperature revealed an anomaly at about 150 K for RS and DRS (deuterated Rochelle salt), and in the range 150–180 K for NAT crystals (Gaba, Kostetskii & Romanyuk, 1989). The authors drew the conclusion that the anomaly was a result of a structural reconstruction caused mainly by changes within the tartaric anion since neither the isomorphous replacement of K^+ by NH_4^+, nor the deuteration significantly influenced the behaviour of the α_x and α_y coefficients against temperature.

These peculiar physical properties of NAT crystals inspired us to study the crystal structure, not only at RT (Kuroda & Mason, 1981) but also in the whole range of the paraelectric phase, i.e. from RT down to the ferroelectric phase transition. Furthermore, we found it worthwhile to examine the structure of NAT crystals in terms of helical atomic arrangements possibly responsible for the optical activity corresponding to the main gyration-tensor components.

Experimental

NAT crystals were grown at room temperature from an aqueous solution of a stoichiometric mixture of disodium (+)-tartrate dihydrate and diammonium (+)-tartrate in an ammonia/air atmosphere. The appropriate tartrates were obtained by reacting sodium and ammonium carbonates, respectively, with (+)-tartaric acid [$NaCO_3$ c.p., $(NH_4)_2CO_3$ p.a.

Table 1. *Important papers on studies of NAT crystals*

Indication of the first-order ferroelectric phase transition (PT)

		Physical property studied	Temperature of PT (K)
Jona & Pepinsky	1953	Dielectric constants ε_a, ε_b and ε_c *versus* temperature (T)	109
Takagi & Makita	1958	Pyroelectric charge *versus* T	109
Gladkii *et al.*	1977	Piezoelectric coefficient $d = P_i/\sigma_\lambda$ *versus* T	113
	1978	Coefficients of elasticity s_{44}, s_{55} and s_{66} *versus* T	113
	1980	Macroscopic quadrupole moment q_μ *versus* T	113
Ivanov *et al.*	1979	Changes of birefringence $\delta(\Delta n)_1$, $\delta(\Delta n)_2$ and $\delta(\Delta n)_3$ *versus* T at $\lambda = 500$ nm	111.8
		Piezoelectric coefficient d_{25} *versus* T	111.5
		Piezooptic effect	112.2
Gaba *et al.*	1983	Refractive indices and birefringence *versus* T	110
Latush *et al.*	1987	Low-frequency $X(ZY)Z$ Raman spectra *versus* T of single crystal	112
Gerbaux *et al.*	1989	Far-IR spectra for a single crystal oriented along a (on heating)	113.8
Gaba *et al.*	1989	Linear thermal-expansion coefficients α_1 and α_2 *versus* T	110

Behaviour of some optical parameters in the paraelectric phase

Gaba *et al.*	1980	$2V$ angle between optic axes *versus* T at $\lambda = 632.8$ and 441.6 nm	150 and 218
Romanyuk *et al.*	1981	Birefringence Δn_1, Δn_2 and Δn_3 *versus* T at $\lambda = 700$ nm	153
Koralewski & Szafrański	1988	Optical rotation ρ (mm^{-1}) along optic axis *versus* T at $\lambda = 632.8$ nm	151

Theoretical explanations of the first-order PT and predictions of structural changes

Aizu	1971, 1984, 1986a,b, 1990
Sawada & Takagi	1972
Ishibashi & Takagi	1975
Sannikov & Levanyuk	1977

Crystal structure of the paraelectric phase

Beevers & Hughes	1941
Shkuratova *et al.*	1979
Kuroda & Mason	1981

Preliminary X-ray investigations of the ferroelectric phase

Sawada & Takagi	1971
Iizumi & Gesi	1978

and (+)-tartaric acid c.p.; Polskie Odczynniki Chemiczne], and then recrystallizing from aqueous solutions. The specific rotation of an aqueous solution of the tartaric acid used was measured with a Polamat-A spectropolarimeter at a few concentrations. In general, it was found to be dextrorotatory, although it can change sign as a function of the wavelength and/or concentration of the solution (Fig. 1). This is consistent with published data (Lowry, 1964).
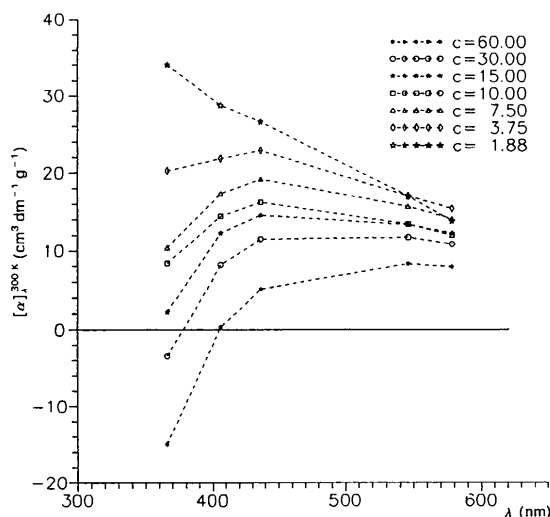

Fig. 1. Dispersion of the specific rotation $[\alpha]_\lambda^{300K} = 100\alpha/lc$ for (+)-tartaric acid aqueous solutions at different concentrations [l is the path length in dm and c the concentration of (+)-tartaric acid in g per 100 cm of solution]. The experimental resolution was estimated as $0.1°$ cm^3 dm^{-1} g^{-1}.

A single colourless NAT crystal of good optical quality with dimensions 0.38 (1) × 0.38 (1) × 0.38 (1) mm was cut and mounted on a glass capillary. The crystal was then coated with silicon oil, since it is very hygroscopic in a humid environment whereas it loses water and/or ammonia easily in a dry atmosphere. Data collections at 295, 200, 151 and 120 K were carried out on a Stoe Stadi-4 diffractometer (graphite-monochromated Cu $K\alpha$* radiation) with an Oxford Cryostream cooler (pure dry nitrogen-gas stream; temperature stability ± 0.1 K). The cooler was calibrated for phase transitions of langbeinite, 88 K, hexamethylbenzene, 111 K, and for RT and higher temperatures with a thermistor thermometer placed on the goniometer head instead of a crystal (Glazer & Cosier, 1990). Also, for the NAT crystal itself the temperature of the ferroelectric phase transition has been confirmed as 110 K on cooling down to 85 K (an approach towards the structure analysis of the ferroelectric phase has been made; see *Appendix* 1). The structure at 295 K [$a = 12.1719$ (5), $b = 14.4043$ (33), $c = 6.2290$ (3) Å, $V = 1092$ (1) Å^3, $D_x = 1.588$, $Z = 4$, $P2_12_12$] agreed essentially with that published by Kuroda & Mason (1981), so it is not reported here. Details of the data collections and structure refinements below room temperature, performed with the *SHELX*76 program (Sheldrick, 1976), are given in Table 2. The data were corrected for Lorentz, polarization and absorption (empirical absorption correction using a ψ scan on six chosen reflections) effects. Atomic scattering factors for neutral atoms were taken from *International Tables for X-ray Crystallography* (1974, Vol. IV). The positional and anisotropic thermal parameters of non-H atoms, together with the positional and isotropic thermal parameters for H atoms, were refined. Geometric calculations were carried out

---

* Cu $K\alpha$ radiation was chosen to control the absolute structure of the NAT crystal during the whole experiment.

Table 2. *Summary of data collection and structure refinement of* $NaNH_4[(2R,3R)-C_4H_4O_6].4H_2O$

$(M_r = 261.16)$

	200 K	151 K	120 K
Space group	$P2_12_12$	$P2_12_12$	$P2_12_12$
Lattice-parameter measurements (Å)	12.112 (1), 14.310 (17), 6.204 (1)	12.088 (2), 14.281 (31), 6.192 (1)	12.065 (6), 14.346 (7), 6.165 (3)
θ range (°)	$38 < \theta < 41$	$38 < \theta < 41$	$28 < \theta < 30$
No. of reflections	13	15	16
V (Å³), Z, D_x (Mg m⁻³)	1075 (1), 4, 1.613	1069 (2), 4, 1.623	1067 (1), 4, 1.626
Intensity measurements			
θ range (°), No. of unique sets	$3 \leq \theta \leq 60$, 2	$3 \leq \theta \leq 60$, 2	$3 \leq \theta \leq 60$, 2
Maximum hkl	13, 16, 6	13, 16, 6	13, 16, 6
Scan mode	$\omega/2\theta$	$\omega/2\theta$	$\omega'2\theta$
Intensity control reflections			
measured every hour	241, 440 and 331	241, 440 and 331	241, 440 and 331
Changes in intensity (%)	± 1.3	± 2.9	± 2.6
No. of reflections measured	2901	3066	2920
Criterion for observed reflections	$\|F_o\| \geq 3\sigma(F_o)$	$F_o \geq 3\sigma(F_o)$	$F_o \geq 3\sigma(F_o)$
No. of observed unique reflections including Friedel opposites, R_{int}	1220, 0.0516	1221, 0.0476	1216, 0.0581
Linear absorption coefficient μ (cm⁻¹)	17.11	17.22	17.20
Max., min. transmission factors	0.4092, 0.6238	0.4091, 0.6239	0.4089, 0.6240
Refinement method	Full-matrix least squares on F_o's	Full-matrix least squares on F_o's	Full-matrix least squares on F_o's
No. of parameters refined	211	211	211
Extinction parameter ($SHELX76$)	0.0404 (8)	0.0425 (12)	0.0233 (8)
$w = [\sigma^2(F_o) + g(F_o)^2]^{-1}$			
g converged to	0.001713	0.002403	0.002852
R, R_w, wR, S	0.0344, 0.0410, 0.0537, 1.257	0.0334, 0.0379, 0.0499, 0.995	0.0376, 0.0408, 0.0527, 0.965
Δ/σ average, max.			
Non-H atoms	0.02, 0.11	0.02, 0.09	0.02, 0.10
H atoms*	0.09, 0.63	0.08, 0.43	0.12, 0.87
Max., min. height in final difference Fourier map (e Å⁻³)	0.14, −0.18	0.18, −0.26	0.23, −0.25
For anti-structure ($\bar{x}\bar{y}\bar{z}$) $NaNH_4[(2S,3S)-C_4H_4O_6].4H_2O$			
R, R_w, wR, S	0.0351, 0.0427, 0.0560, 1.310	0.0341, 0.0395, 0.0519, 1.034	0.0382, 0.0424, 0.0544, 0.995

* Initial positional H-atom parameters from the difference Fourier map.

using the *PARST* program (Nardelli, 1983) and drawings were made with *ORTEP*II (Johnson, 1971).

Discussion

The absolute structure of the crystals investigated has been established in two ways: (i) a dextrorotatory aqueous solution of the natural L-(+)-tartaric acid (*i.e.* of configuration $2R,3R$) was used to obtain the NAT crystals; (ii) R factors for the anti-structure, resulting in the configuration $2S,3S$ of the tartaric anion, were always greater than those for the $2R,3R$ structure (Table 2). The final atomic coordinates and equivalent isotropic thermal parameters at 200, 151 and 120 K are listed in Table 3.* The numbering of atoms in the $[(2R,3R)-C_4H_4O_6]^{2-}$ anion is shown in Fig. 2. Bond lengths and Na—O contacts as well as bond and torsion angles are given in Table 4.

The large number of potential donors for hydrogen bonding together with available acceptors in the asymmetric unit results in a complex hydrogen-bond network (Table 5). The O atoms of both carboxyl groups, which are in close contact with the Na⁺

cation, also interact with a pair of H-atom donors each. The two remaining carboxyl O atoms, O(2) and O(6), both accept three hydrogen bonds [the set of donors for O(2) is different from that for O(6)]. The hydroxyl O(3) atom donates an intramolecular hydrogen bond, whereas the hydroxyl O(4) atom forms a bifurcated hydrogen bond with the carboxyl O(5) within the same molecule and with O(5W) ($x + \frac{1}{2}, -y + \frac{3}{2}, -z + 1$). The twofold symmetry expected for a free tartaric anion of $2R,3R$ configuration is thus lost. It can be seen from Table 5 that the O(4)···O(5) intramolecular component of the bifurcated hydrogen-bond weakens with decreasing temperature (notice the systematic change of the O—H···O angle). In contrast, because of the contraction of the structure, the O(4)···O(5W) intermolecular component becomes linear and dominating. It means that at 150 K and below, the hydrogen bond is no longer bifurcated. This is accompanied by a change of the H(O4)—O(4)—C(3)—C(4) torsion angle from $-7°$ at RT to $-56°$ at 120 K (Table 4). The most significant change we observed was at 151 K.

The symmetry and conformation of the $[(2R,3R)-C_4H_4O_6]^{2-}$ anion are consistent with those observed in hydrogen-rich structures of other tartrates, *e.g.* DKT: $K_2(2R,3R)-C_4H_4O_6.0.5H_2O$, KHT: $K[(+)-C_4H_5O_6]$ and (+)-tartaric acid itself, for which values of the appropriate torsion angles were listed in the paper of Stadnicka & Brożek (1991).

---

* Lists of structure factors, anisotropic thermal parameters and H-atom parameters as well as Table $A2$ have been deposited with the British Library Document Supply Centre as Supplementary Publication No. SUP 71238 (28 pp.). Copies may be obtained through The Technical Editor, International Union of Crystallography, 5 Abbey Square, Chester CH1 2HU, England. [CIF reference: AB0306]

Table 3. *Fractional atomic coordinates, equivalent isotropic parameters,* U_{eq} (Å^2), *with e.s.d.'s in parentheses and relative displacement parameters*

$$U_{eq} = (1/3)\Sigma_i \Sigma_j U_{ij} a_i^* a_j^* \mathbf{a}_i . \mathbf{a}_j.$$

	x	y	z	U_{eq}	$(U_{11}/U_{22})^{1/2}$	$(U_{11}/U_{33})^{1/2}$	$(U_{33}/U_{22})^{1/2}$
200 K							
Na	0.73013 (7)	0.49153 (6)	0.51326 (15)	0.0206 (2)	1.41	1.10	1.28
O(1)	0.6214 (1)	0.6102 (1)	0.3492 (3)	0.0216 (3)	1.38	1.13	1.23
O(2)	0.7105 (1)	0.7018 (1)	0.1133 (3)	0.0238 (4)	1.37	1.39	0.99
O(3)	0.6729 (1)	0.8560 (1)	0.3239 (3)	0.0215 (3)	1.82	1.49	1.22
O(4)	0.7954 (1)	0.7473 (1)	0.6311 (3)	0.0220 (3)	1.28	1.02	1.25
O(5)	0.7296 (1)	0.9036 (1)	0.8191 (3)	0.0259 (3)	1.39	1.41	0.98
O(6)	0.5541 (1)	0.8584 (1)	0.8391 (3)	0.0269 (4)	1.06	1.11	0.96
C(1)	0.6563 (2)	0.6887 (1)	0.2812 (3)	0.0151 (4)	1.23	1.33	0.92
C(2)	0.6310 (2)	0.7726 (2)	0.4205 (3)	0.0166 (4)	1.41	1.15	1.22
C(3)	0.6805 (2)	0.7629 (1)	0.6436 (4)	0.0186 (4)	1.27	1.37	0.92
C(4)	0.6524 (2)	0.8484 (1)	0.7790 (3)	0.0185 (4)	1.55	1.75	0.88
N(1)	0.5000	0.0000	0.1416 (4)	0.0253 (4)	1.22	1.13	1.09
N(2)	0.5000	0.5000	0.0450 (5)	0.0399 (5)	1.06	1.12	0.94
O(3W)	0.4342 (1)	0.7008 (1)	0.9547 (3)	0.0429 (4)	0.91	0.98	0.92
O(4W)	0.7395 (1)	0.5405 (1)	0.8759 (3)	0.0312 (4)	1.89	1.74	1.09
O(5W)	0.4235 (1)	0.6066 (1)	0.5644 (4)	0.0450 (4)	0.86	0.74	1.17
O(6W)	0.3908 (1)	0.9163 (1)	0.5226 (3)	0.0267 (3)	1.16	0.98	1.18
151 K							
Na	0.73011 (6)	0.49121 (6)	0.51152 (14)	0.0180 (2)	1.40	1.11	1.26
O(1)	0.6211 (1)	0.6106 (1)	0.3485 (3)	0.0174 (4)	1.65	1.29	1.28
O(2)	0.7103 (1)	0.7015 (1)	0.1138 (3)	0.0204 (4)	1.37	1.37	1.00
O(3)	0.6739 (1)	0.8561 (1)	0.3232 (3)	0.0177 (4)	1.95	1.51	1.29
O(4)	0.7960 (1)	0.7471 (1)	0.6333 (3)	0.0185 (4)	1.25	1.03	1.21
O(5)	0.7288 (1)	0.9046 (1)	0.8207 (3)	0.0217 (4)	1.43	1.38	1.03
O(6)	0.5529 (1)	0.8575 (1)	0.8398 (3)	0.0227 (4)	1.18	1.21	0.98
C(1)	0.6560 (2)	0.6882 (1)	0.2802 (4)	0.0147 (5)	1.14	1.20	0.96
C(2)	0.6313 (2)	0.7729 (2)	0.4200 (4)	0.0146 (4)	1.50	1.12	1.33
C(3)	0.6800 (2)	0.7628 (1)	0.6448 (4)	0.0150 (5)	1.28	1.26	1.02
C(4)	0.6522 (2)	0.8481 (1)	0.7808 (4)	0.0151 (5)	1.39	1.56	0.89
N(1)	0.5000	0.0000	0.1422 (5)	0.0199 (5)	1.19	1.03	1.16
N(2)	0.5000	0.5000	0.0400 (5)	0.0358 (6)	1.25	1.16	1.08
O(3W)	0.4351 (1)	0.6991 (1)	0.9566 (3)	0.0340 (5)	0.92	0.92	1.00
O(4W)	0.7388 (1)	0.5401 (1)	0.8746 (3)	0.0270 (4)	1.89	1.98	0.96
O(5W)	0.4224 (1)	0.6085 (1)	0.5638 (3)	0.0347 (5)	0.94	0.76	1.24
O(6W)	0.3898 (1)	0.9168 (1)	0.5219 (3)	0.0211 (4)	1.18	1.04	1.14
120 K							
Na	0.72978 (7)	0.49114 (6)	0.50995 (14)	0.0145 (2)	1.69	1.43	1.18
O(1)	0.6204 (1)	0.6101 (1)	0.3489 (3)	0.0151 (4)	1.64	1.45	1.13
O(2)	0.7108 (1)	0.7015 (1)	0.1120 (3)	0.0168 (4)	1.54	1.71	0.90
O(3)	0.6742 (1)	0.8558 (1)	0.3234 (3)	0.0153 (3)	1.97	1.66	1.19
O(4)	0.7957 (1)	0.7471 (1)	0.6335 (3)	0.0149 (3)	1.52	1.26	1.21
O(5)	0.7279 (1)	0.9044 (1)	0.8220 (3)	0.0180 (3)	1.69	1.80	0.94
O(6)	0.5519 (1)	0.8577 (1)	0.8403 (3)	0.0187 (4)	1.40	1.46	0.96
C(1)	0.6558 (2)	0.6880 (1)	0.2812 (4)	0.0122 (4)	1.25	1.42	0.88
C(2)	0.6308 (2)	0.7732 (2)	0.4200 (4)	0.0123 (4)	1.75	1.35	1.30
C(3)	0.6796 (2)	0.7634 (1)	0.6460 (4)	0.0128 (4)	1.45	1.47	0.99
C(4)	0.6514 (2)	0.8487 (2)	0.7814 (4)	0.0136 (4)	1.21	2.27	0.53
N(1)	0.5000	0.0000	0.1427 (4)	0.0159 (4)	1.44	1.40	1.03
N(2)	0.5000	0.5000	0.0384 (5)	0.0313 (5)	1.22	1.16	1.05
O(3W)	0.4358 (1)	0.6988 (1)	0.9595 (3)	0.0267 (4)	1.06	1.03	1.03
O(4W)	0.7373 (1)	0.5398 (1)	0.8736 (3)	0.0242 (4)	2.09	2.21	0.95
O(5W)	0.4215 (1)	0.6094 (1)	0.5621 (3)	0.0281 (4)	1.02	0.91	1.11
O(6W)	0.3895 (1)	0.9163 (1)	0.5220 (3)	0.0183 (3)	1.36	1.13	1.20

The H atoms of the four symmetry-independent water molecules and the two ammonium cations situated on the twofold axes along [001] all participate in the hydrogen-bond network. They differ in their modes of hydrogen-bond acceptance. O(3W) accepts two H atoms, O(5W) and O(6W) accept only one H atom each, whereas the O(4W) does not act as an acceptor. On the other hand, only the O(3W) atom does not belong to the environment nearest to the Na$^+$ cation.

Inspection of the unit-cell projections along [100], [010] and [001] at different temperatures results in the conclusion that not only a natural contraction of the thermal ellipsoids with decreasing temperature occurs, but also that their orientation changes and a relative elongation takes place in the direction [100]. This can be expressed by the relative displacement parameters, given in Table 3. The average values of the parameters for the non-H atoms are:

	$(U_{11}/U_{22})^{1/2}$	$(U_{11}/U_{33})^{1/2}$	$(U_{33}/U_{22})^{1/2}$
RT	1.22	1.06	1.16
200 K	1.31	1.23	1.07
151 K	1.35	1.23	1.11
120 K	1.49	1.48	1.03

The relative elongation in the [100] direction increases rapidly between 151 and 120 K. Moreover, strong light scattering was observed long before approaching the ferroelectric phase transition during measurements of ORP along the optical axis for NAT crystals with decreasing temperature

Table 4. $[(2R,3R)\text{-}C_4H_4O_6]^{2-}$ *bond lengths and* Na—O *contacts* (Å), *bond angles and torsion angles* (°) *with e.s.d.'s in parentheses*

	Room temperature*	200 K	151 K	120 K
O(1)—C(1)	1.269 (4)	1.272 (3)	1.259 (3)	1.268 (3)
O(2)—C(1)	1.240 (5)	1.245 (2)	1.236 (3)	1.251 (3)
O(3)—C(2)	1.419 (5)	1.429 (3)	1.428 (3)	1.426 (3)
O(4)—C(3)	1.415 (4)	1.412 (3)	1.423 (3)	1.423 (3)
O(5)—C(4)	1.260 (5)	1.251 (3)	1.254 (3)	1.246 (3)
O(6)—C(4)	1.247 (6)	1.256 (3)	1.261 (3)	1.262 (3)
C(1)—C(2)	1.537 (5)	1.510 (3)	1.518 (4)	1.522 (3)
C(2)—C(3)	1.529 (5)	1.515 (3)	1.518 (3)	1.519 (3)
C(3)—C(4)	1.532 (5)	1.522 (3)	1.518 (4)	1.520 (3)
Na—O(1)	2.396 (3)	2.379 (2)	2.379 (3)	2.375 (2)
Na—O(4W)	2.366 (4)	2.359 (2)	2.357 (2)	2.350 (2)
Na—O(3')	2.505 (3)	2.482 (3)	2.473 (4)	2.484 (2)
Na—O(5')	2.478 (4)	2.463 (2)	2.451 (2)	2.449 (2)
Na—O(5W'')	2.353 (4)	2.353 (2)	2.352 (3)	2.349 (2)
Na—O(6W''')	2.372 (3)	2.362 (2)	2.344 (2)	2.349 (2)
O(1)—C(1)—O(2)	126.4 (3)	125.8 (3)	126.4 (4)	126.2 (2)
O(1)—C(1)—C(2)	116.6 (3)	116.4 (2)	116.4 (2)	117.1 (2)
O(2)—C(1)—C(2)	117.0 (3)	117.8 (2)	117.2 (3)	116.8 (2)
O(3)—C(2)—C(1)	110.9 (3)	110.6 (2)	110.7 (2)	111.1 (2)
O(3)—C(2)—C(3)	109.6 (3)	108.7 (2)	108.9 (3)	108.5 (2)
O(4)—C(3)—C(2)	110.3 (3)	110.7 (2)	110.6 (2)	110.3 (2)
O(4)—C(3)—C(4)	11.8 (3)	112.2 (2)	111.9 (2)	112.4 (2)
C(1)—C(2)—C(3)	110.4 (3)	111.7 (2)	111.8 (3)	111.4 (2)
C(2)—C(3)—C(4)	109.5 (3)	110.0 (2)	110.3 (2)	110.0 (2)
O(5)—C(4)—O(6)	125.5 (3)	125.2 (3)	125.3 (3)	125.6 (2)
O(5)—C(4)—C(3)	117.0 (4)	116.9 (2)	117.5 (2)	117.5 (2)
O(6)—C(4)—C(3)	117.5 (5)	117.8 (2)	117.2 (2)	116.9 (2)
O(1)—C(1)—C(2)—O(3)	− 178.5 (3)	− 178.9 (2)	− 179.3 (3)	179.3 (2)
O(2)—C(1)—C(2)—O(3)	1.3 (5)	2.3 (3)	2.3 (4)	1.6 (3)
O(1)—C(1)—C(2)—C(3)	59.9 (4)	60.0 (3)	59.2 (4)	59.6 (3)
O(2)—C(1)—C(2)—C(3)	− 120.4 (4)	− 118.9 (3)	− 119.3 (3)	− 119.5 (2)
H(O3)—O(3)—C(2)—C(1)	− 16 (4)	− 3.2 (9)	−9 (1)	− 18.9 (7)
C(1)—C(2)—C(3)—O(4)	56.7 (4)	55.8 (3)	56.5 (4)	56.3 (3)
O(3)—C(2)—C(3)—O(4)	− 65.7 (4)	− 66.5 (3)	− 66.1 (4)	− 66.2 (2)
C(1)—C(2)—C(3)—C(4)	− 179.8 (3)	− 179.6 (2)	179.5 (3)	− 179.1 (2)
O(3)—C(2)—C(3)—C(4)	57.8 (4)	58.1 (3)	58.3 (4)	58.4 (2)
O(6)—C(4)—C(3)—O(4)	− 166.6 (3)	− 165.5 (2)	− 165.5 (3)	− 165.4 (2)
O(5)—C(4)—C(3)—O(4)	15.2 (5)	15.3 (3)	16.3 (4)	15.7 (3)
O(6)—C(4)—C(3)—C(2)	70.9 (4)	70.8 (3)	71.0 (4)	71.2 (3)
O(5)—C(4)—C(3)—C(2)	− 107.3 (4)	− 108.4 (3)	− 107.2 (4)	− 107.7 (3)
H(O4)—O(4)—C(3)—C(4)	− 7 (4)	− 36.1 (9)	− 55 (1)	− 56.3 (8)

Dihedral angle between planes O(1)O(2)C(1)C(2)O(3) and O(4)C(3)C(4)O(5)O(6)

51.4 (1)	51.08 (7)	51.14 (9)	50.80 (7)

Symmetry codes: (i) $-x + \frac{3}{2}, y - \frac{1}{2}, -z + 1$; (ii) $-x + 1, -y + 1, z$; (iii) $x + \frac{1}{2}, -y + \frac{1}{2}, -z + 1$.

*Data at room temperature taken from Kuroda & Mason (1981).

(Koralewski, 1991). This may suggest a preparation for the ferroelectric phase transition which would begin as high as about 150 K. The elongation seems to lead to doubling of the unit-cell parameter a in the ferroelectric phase below 110 K, detected by Sawada & Takagi (1972) and the present authors (*Appendix* 1). The phenomenon of thermal-ellipsoid elongation has already been claimed for the paraelectric phase of Rochelle salt just above the ferroelectric phase transition at 297 K (Iwata, Koyano & Shibuya; 1989) and in the low-temperature non-polar phase of Rochelle salt at 78 K (Iwata, Mitani, Fukui & Shibuya; 1989). However, the elongation can also be considered to result from an additional phase transition (at a temperature higher than 110 K) to an

intermediate non-ferroelectric incommensurate phase. The changes in the crystal structure at 30–40 K above 110 K are consistent with the behaviour of some optical parameters around 150 K (Table 1).

Inquiry into the shortest distances between highly polarizable atoms (Glazer & Stadnicka, 1986) reveals three intermolecular helices: one non-symmetric, LS4/4, along c, and two symmetric, RS3/6 and LS3/4, along b and a, respectively (Table 6 and Fig. 3). Since within a chosen section of helix the expected polarizability ellipsoids have alternating radial and tangential alignment and sometimes even an iso-tropic cross-section, it is difficult to predict the sign of the ORP. Nevertheless, for all the helices the contribution of atoms with radial polarizability ellipsoids prevails and so accounts for the negative sign of optical rotation in the case of LS4/4 and LS3/4 and the positive sign in the case of RS3/6.

The components of the gyration tensor for NAT crystals have been estimated earlier taking into account the dispersion of optical rotation along one of the optical axes with both wavelength and temperature (Koralewski & Szafrański, 1988). Considering the observed pseudo-uniaxial state ($2V = 0$ for $T = 151$ K and $\lambda = 632.8$ nm) as well as the change of the plane of the optical axes (from bc for $T > 151$ K to ac for $T < 151$ K) and making the assumption of a negligible temperature influence on the gyration tensor, the values $g_{11} = 18\ (3) \times 10^{-6}$, $g_{22} = -28\ (4) \times 10^{-6}$ and $g_{33} = 65\ (2) \times 10^{-7}$ were calculated by these authors. It should be pointed out
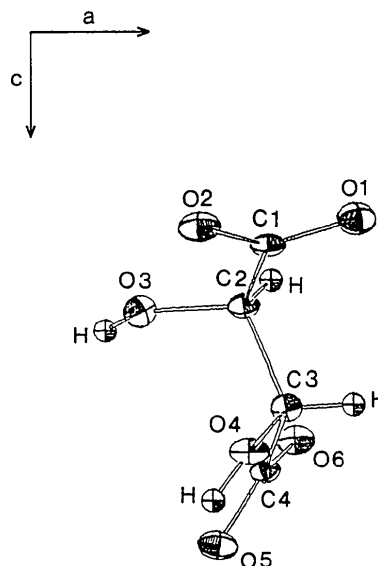

Fig. 2. Numbering of atoms in the $(2R,3R)$-tartaric anion shown for the projection along [010] at 151 K. Atoms are represented by thermal ellipsoids at the 50% probability level.

Table 5. *Geometry of hydrogen-bonding in NAT crystal structures at room temperature, 200, 151 and 120 K*

D—H···A	A Symmetry code	D···A (Å)	D—H (Å)	H···A (Å)	D—H···A (°)
Room temperature*					
O(3)—H(O3)···O(2)	x, y, z	2.614 (4)	0.95 (6)	2.06 (7)	116 (5)
O(4)—H(O4)···O(5)	x, y, z	2.656 (4)	0.99 (8)	1.96 (8)	125 (6)
O(4)—H(O4)···O(5W)	x + ½, -y + ½, -z + 1	2.955 (5)	0.99 (8)	2.49 (8)	108 (5)
O(3W)—H(3W1)···O(6)	x, y, z	2.796 (5)	0.93 (6)	1.99 (6)	144 (6)
O(3W)—H(3W2)···O(2)	x - ½, -y + ½, -z + 1	3.067 (5)	0.93 (6)	2.14 (6)	171 (6)
O(4W)—H(4W1)···O(2)	x, y, z + 1	2.772 (4)	0.86 (10)	1.96 (10)	156 (7)
O(4W)—H(4W2)···O(5)	-x + ½, y - ½, -z + 2	2.748 (4)	0.91 (7)	1.85 (7)	168 (6)
O(5W) - H(5W1)···O(3W)	x, y, z	2.786 (7)	0.97 (1)	1.82 (6)	173 (5)
O(5W)—H(5W2)···O(1)	x, y, z	2.756 (5)	0.91 (8)	2.01 (8)	139 (6)
O(6W)—H(6W1)···O(6)	x, y, z	2.940 (5)	1.01 (5)	2.10 (7)	139 (4)
O(6W)—H(6W2)···O(4)	x - ½, -y + ½, -z + 1	2.792 (4)	0.95 (7)	1.92 (7)	152 (7)
N(1)—H(N11)···O(6W)	-x + 1, -y + 1, z	2.973 (6)	1.0 (2)	2.1 (3)	156 (7)
N(1)—H(N12)···O(6)	-x + 1, -y + 1, z - 1	2.855 (5)	1.1 (7)	1.8 (7)	160 (8)
N(2)—H(N21)···O(3W)	-x + 1, -y + 1, z - 1	3.108 (5)	1.11 (7)	2.13 (7)	146 (6)
N(2)—H(N22)···O(1)	x, y, z	2.873 (6)	1.01 (7)	1.90 (7)	160 (6)
200 K					
O(3)—H(O3)···O(2)	x, y, z	2.605 (3)	0.69 (1)	2.20 (1)	119 (1)
O(4)—H(O4)···O(5)	x, y, z	2.649 (3)	0.72 (1)	2.37 (1)	105 (1)
O(4)—H(O4)···O(5W)	x + ½, -y + ½, -z + 1	2.872 (3)	0.72 (1)	2.22 (1)	150 (1)
O(3W)—H(3W1)···O(6)	x, y, z	2.777 (3)	1.12 (1)	1.70 (1)	159 (1)
O(3W)—H(3W2)···O(2)	x - ½, -y + ½, -z + 1	3.075 (3)	0.91 (1)	2.20 (1)	162 (1)
O(4W)—H(4W1)···O(2)	x, y, z + 1	2.761 (3)	0.83 (1)	1.94 (1)	174 (1)
O(4W)—H(4W2)···O(5)	-x + ½, y - ½, -z + 2	2.649 (3)	0.91 (1)	2.20 (1)	162 (1)
O(5W)—H(5W1)···O(3W)	x, y, z	2.774 (3)	0.93 (1)	1.83 (1)	167 (1)
O(5W)—H(5W2)···O(1)	x, y, z	2.744 (2)	0.80 (1)	1.97 (1)	165 (1)
O(6W)—H(6W1)···O(6)	x, y, z	2.907 (2)	0.98 (1)	1.97 (1)	160 (1)
O(6W)—H(6W2)···O(4)	x - ½, -y + ½, -z + 1	2.779 (3)	0.84 (1)	1.95 (1)	169 (1)
N(1)—H(N11)···O(6W)	-x + 1, -y + 1, z	2.962 (3)	0.80 (1)	2.38 (1)	130 (1)
N(1)—H(N12)···O(6)	-x + 1, -y + 1, z - 1	2.839 (3)	1.12 (1)	1.74 (1)	167 (1)
N(2)—H(N21)···O(3W)	-x + 1, -y + 1, z - 1	3.034 (4)	0.99 (1)	2.16 (1)	146 (1)
N(2)—H(N22)···O(1)	x, y, z	2.865 (3)	0.80 (1)	2.11 (1)	158 (1)
151 K					
O(3)—H(O3)···O(2)	x, y, z	2.598 (5)	0.86 (1)	2.10 (2)	116 (1)
O(4)—H(O4)···O(5)	x, y, z	2.880 (3)	0.86 (1)	2.49 (1)	92 (1)
O(4)—H(O4)···O(5W)	x + ½, -y + ½, -z + 1	2.843 (4)	0.86 (1)	2.00 (1)	170 (1)
O(3W)—H(3W1)···O(6)	x, y, z	2.769 (5)	0.75 (1)	2.02 (1)	174 (1)
O(3W)—H(3W2)···O(2)	x - ½, -y + ½, -z + 1	3.097 (3)	0.75 (1)	2.47 (1)	142 (1)
O(4W)—H(4W1)···O(2)	x, y, z + 1	2.761 (5)	0.94 (1)	1.82 (2)	178 (1)
O(4W)—H(4W2)···O(5)	-x + ½, y - ½, -z + 2	2.731 (4)	0.98 (1)	1.76 (1)	170 (1)
O(5W)—H(5W1)···O(3W)	x, y, z	2.759 (3)	1.02 (1)	1.74 (1)	172 (1)
O(5W)—H(5W2)···O(1)	x, y, z	2.747 (2)	0.78 (1)	1.99 (1)	165 (1)
O(6W)—H(6W1)···O(6)	x, y, z	2.912 (2)	0.91 (1)	2.02 (1)	170 (1)
O(6W)—H(6W2)···O(4)	x - ½, -y + ½, -z + 1	2.771 (5)	0.93 (2)	1.89 (2)	159 (1)
N(1)—H(N11)···O(6W)	-x + 1, -y + 1, z	2.952 (3)	0.79 (1)	2.30 (1)	140 (1)
N(1)—H(N12)···O(6)	-x + 1, -y + 1, z - 1	2.839 (4)	0.88 (1)	1.99 (1)	163 (1)
N(2)—H(N21)···O(3W)	-x + 1, -y + 1, z - 1	2.994 (6)	1.05 (2)	2.02 (2)	154 (1)
N(2)—H(N22)···O(1)	x, y, z	2.879 (3)	0.89 (1)	2.00 (1)	167 (1)
120 K					
O(3)—H(O3)···O(2)	x, y, z	2.606 (2)	0.88 (1)	2.11 (1)	115 (1)
O(4)—H(O4)···O(5)	x, y, z	2.666 (2)	0.74 (1)	2.52 (1)	93 (1)
O(4)—H(O4)···O(5W)	x + ½, -y + ½, -z + 1	2.828 (2)	0.74 (1)	2.09 (1)	173 (1)
O(3W)—H(3W1)···O(6)	x, y, z	2.773 (2)	1.10 (1)	2.00 (1)	125 (1)
O(3W)—H(3W2)···O(2)	x - ½, -y + ½, -z + 1	3.100 (3)	0.82 (1)	2.29 (1)	169 (1)
O(4W)—H(4W1)···O(2)	x, y, z + 1	2.765 (2)	0.89 (1)	1.88 (1)	172 (1)
O(4W)—H(4W2)···O(5)	-x + ½, y - ½, -z + 2	2.734 (3)	1.06 (1)	1.68 (1)	174 (1)
O(5W)—H(5W1)···O(3W)	x, y, z	2.771 (3)	0.82 (1)	1.95 (1)	178 (1)
O(5W)—H(5W2)···O(1)	x, y, z	2.736 (3)	0.81 (1)	1.93 (1)	178 (1)
O(6W)—H(6W1)···O(6)	x, y, z	2.897 (2)	0.83 (1)	2.07 (1)	171 (1)
O(6W)—H(6W2)···O(4)	x - ½, -y + ½, -z + 1	2.773 (2)	0.92 (1)	1.88 (1)	166 (1)
N(1)—H(N11)···O(6W)	-x + 1, -y + 1, z	2.947 (3)	0.81 (1)	2.25 (1)	144 (1)
N(1)—H(N12)···O(6)	-x + 1, -y + 1, z - 1	2.835 (2)	1.02 (1)	1.84 (1)	165 (1)
N(2)—H(N21)···O(3W)	-x + 1, -y + 1, z - 1	2.995 (2)	0.87 (1)	2.24 (2)	146 (1)
N(2)—H(N22)···O(1)	x, y, z	2.876 (3)	0.84 (1)	2.08 (1)	157 (1)

* Data at room temperature are taken from Kuroda & Mason (1981).

that these results were obtained for an NAT crystal with tartaric anions of 2S,3S configuration (see *Appendix* 2). Thus, the qualitative structural prediction of the optical-rotation sign along [100], [010] and [001] for our NAT crystal is consistent with the absolute structure determined. The appropriate measurements of the optical rotation at room temperature along **a**, **b** and **c**, *i.e.* in the directions where it is predominated by the effect of linear birefringence, are in progress using the high accuracy ultrapolarimeter in collaboration with the Clarendon Laboratory, Oxford University, England.

Table 6. *Helical atomic arrangements along* [001], [010] *and* [100] *directions*

Data are given for room temperature.* d is the distance between adjacent atoms.

	Symmetry code	z	d (Å)
LS4/4 along c			
O(3W)	$x + \frac{1}{2}, -y + \frac{1}{2}, -z + 1$	0.0493	
			2.796 (5)
O(6)	$x + \frac{1}{2}, -y + \frac{1}{2}, -z + 1$	0.1637	
			2.940 (5)
O(6W)	$x + \frac{1}{2}, -y + \frac{1}{2}, -z + 1$	0.4805	
			2.792 (4)
O(4)	x, y, z	0.6298	
			3.183 (6)
O(3W)	$x + \frac{1}{2}, -y + \frac{1}{2}, -z + 2$	1.0493	
RS3/6 along b			
O(3)	$-x + 1, -y + 1, z + 1$	0.1449	
			2.614 (4)
O(2)	$-x + 1, -y + 1, z + 1$	0.2993	
			2.772 (4)
O(4W)	$-x + 1, -y + 1, z$	0.4601	
			3.122 (4)
O(3)	$x - \frac{1}{2}, -y + \frac{1}{2}, -z + 1$	0.6449	
			2.614 (4)
O(2)	$x - \frac{1}{2}, -y + \frac{1}{2}, -z + 1$	0.7993	
			2.772 (4)
O(4W)	$x - \frac{1}{2}, -y + \frac{1}{2}, -z + 2$	0.9601	
			3.122 (4)
O(3)	$-x + 1, -y + 2, z + 1$	1.1449	
LS3/4 along a			
N(2)	$x - \frac{1}{2}, -y + \frac{1}{2}, -z$	0.0000	
			3.188 (4)
O(4W)	$x - \frac{1}{2}, -y + \frac{1}{2}, -z + 1$	0.2424	
			3.190 (4)
N(1)	x, y, z	0.5000	
			3.190 (4)
O(4W)	$-x + \frac{1}{2}, y - \frac{1}{2}, -z + 1$	0.7576	
			3.188 (4)
N(2)	$x + \frac{1}{2}, -y + \frac{1}{2}, -z$	1.0000	

* Atomic coordinates are taken from Kuroda & Mason (1981).

APPENDIX 1

An attempt was made to investigate the NAT crystal structure in the ferroelectric phase. The crystal has passed the phase transition at 110 K with a slow cooling rate, 2 K h^{-1}. The unit-cell parameters at 85 K, Cu $K\alpha$, were found to be $a = 12.055\,(24)$, $b = 14.346\,(34)$ and $c = 6.165\,(3)$ Å, $\alpha = 90.0\,(1)$, $\beta = 91.1\,(1)$ and $\gamma = 90.0\,(2)°$. Data collection was performed but the structure refinement was not satisfactory (R factors about 10%). Some reflections were split or moved away from the Bragg positions in reciprocal space because of the expected twinning (Sawada & Takagi, 1971) as well as a structure modulation below the phase transition (Iizumi & Gesi, 1978). The intensity distribution was later checked for another crystal in the $hk0$, $h0l$ and $0kl$ reciprocal layers every 0.1 fraction of a^*, b^* and c^* [at 90 K, Mo $K\alpha$, the unit-cell parameters were $a = 12.152\,(37)$, $b = 14.390\,(77)$ and $c = 6.184\,(39)$ Å, $\alpha = 90.0\,(5)$, $\beta = 91.1\,(4)$ and $\gamma = 90.0\,(5)°$]. The most informative part was the projection $hk0$ (Fig. 4a) confirming twinning [split reflections (1,2,0), (2,4,0) etc.] and superlattice reflections [(3½,1,0), (3½,3,0), (2½,3,0), (3½,2,0), (3½,4,0), (2½,4,0)], possibly indicating doubling of the parameter a. On the other hand, the detailed structure of the reflection (2,1,0) (Fig. 4b) clearly shows two satellites of $(h \pm \delta,k,0)$ type and the shape of the superlattice reflections does not exclude similar satellites of $(h + \frac{1}{2} \pm \delta,k,0)$ type. The
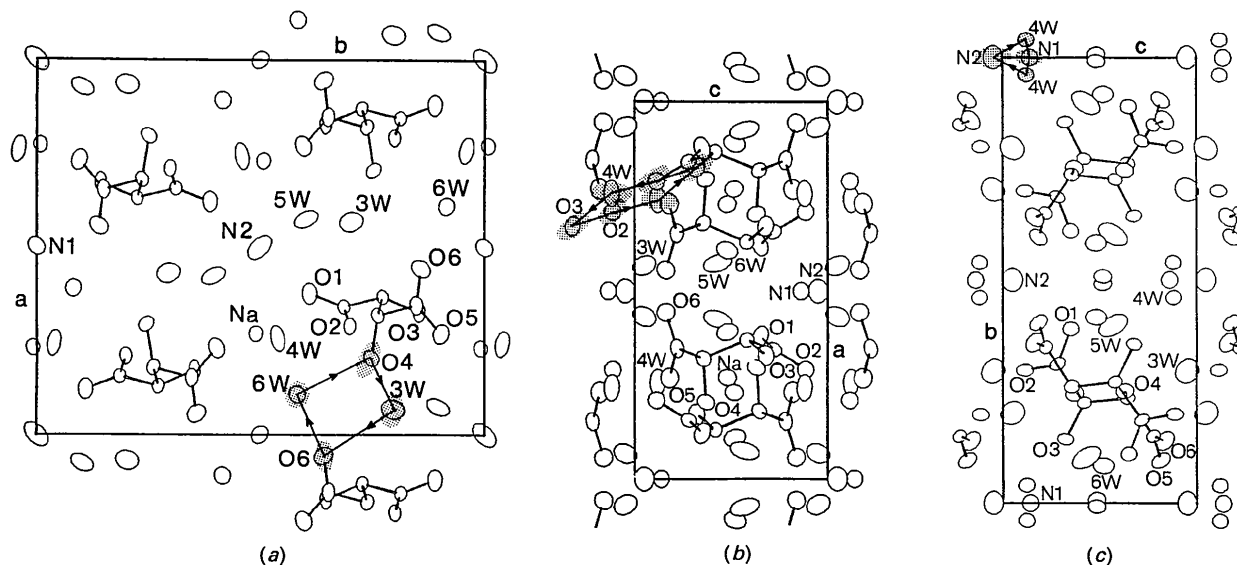

Fig. 3. The helical arrangements of atoms shown in the projections along (a) [001], (b) [010] and (c) [100] for the structure at room temperature (Kuroda & Mason, 1981). Atoms are represented by thermal ellipsoids at the 50% probability level. For the atoms contributing to the helices, polarizability ellipsoids are schematically marked by dashed regions.
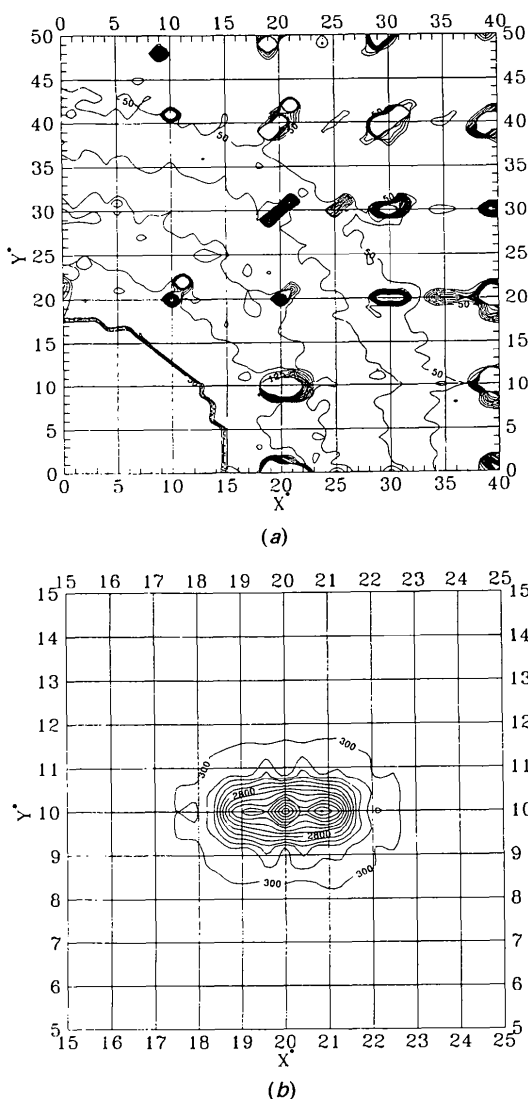
(a)

(b)

Fig. 4. (a) Intensity distribution in the hk0 reciprocal layer at 90 K. The measurement was carried out every $0.1a^*$ and $0.1b^*$. One division of X^* corresponds to 0.00823 Å $^{-1}$ and 0.006949 Å $^{-1}$ for Y^*. (b) Detailed structure of the (2,1,0) reflection together with the satellite reflections $(2 - \delta,1,0)$ and $(2 + \delta,1,0)$ for comparison with the results of Iizumi & Gesi (1978).

positions of the satellite reflections are similar to the neutron scattering results of Iizumi & Gesi (1978) for the deuterated NAT crystal. The superlattice reflection between (1,1,0) and (2,1,0) was not observed for the NAT crystal in our experiment.

APPENDIX 2

The absolute structure of the NAT crystal, used by Koralewski & Szafrański (1988) for optical investigations, has been found to be opposite to that of our crystal. For a fragment of Koralewski's crystal a set

of Bijvoet pairs was measured at room temperature with a KM-4 diffractometer (Kuma Diffraction) using Cu $K\alpha$ graphite-monochromated radiation and the Bijvoet differences (after averaging appropriate groups of measured symmetrically-related reflections) were compared with those calculated from Kuroda & Mason's structural data (Table $A2$, deposited). Among 31 pairs, chosen for $|\Delta F_c/|F_c|| \geq 0.01$, 18 were of the opposite sign, eight of the same sign and five could not be compared since one component of each pair was inaccessible.

References

AIZU, K. (1971). *J. Phys. Soc. Jpn*, **31**, 1521–1526.
AIZU, K. (1984). *J. Phys. Soc. Jpn*, **53**, 1775–1782.
AIZU, K. (1986a). *J. Phys. Soc. Jpn*, **55**, 1663–1670.
AIZU, K. (1986b). *J. Phys. Soc. Jpn*, **55**, 4302–4308.
AIZU, K. (1990). *J. Phys. Soc. Jpn*, **59**, 1293–1298.
BEEVERS, C. A. & HUGHES, W. (1941). *Proc. R. Soc. London, Ser. A*, **177**, 251–259.
GABA, V. M., KOSTETSKII, A. M. & ROMANYUK, N. A. (1980). *Ukr. Fiz. Zh.* **25**, 1208–1209.
GABA, V. M., KOSTETSKII, A. M. & ROMANYUK, N. A. (1989). *Kristallografiya*, **34**, 1041–1043.
GABA, V. M., ZHELUDEV, I. S., KOSTETSKII, A. M. & ROMANYUK, N. A. (1983). *Izv. Akad. Nauk SSSR Ser. Fiz.* **47**, 633–636.
GERBAUX, X., HADNI, A. & KITADE, A. (1989). *Phys. Status Solidi A*, **115**, 587–597.
GLADKII, V. V., KALLAEV, S. I. & KIRIKOV, V. A. (1980). *Solid State Phys.* **22**, 904–905.
GLADKII, V. V., KIRIKOV, V. A. & MAGATAEV, V. K. (1978). *Kristallografiya*, **23**, 421–422.
GLADKII, V. V., MAGATAEV, V. K. & KIRIKOV, V. A. (1977). *Solid State Phys.* **19**, 1102–1106.
GLAZER, A. M. & COSIER J. (1990). Private communication.
GLAZER, A. M. & STADNICKA, K. (1986). *J. Appl. Cryst.* **19**, 108–122.
IIZUMI, M. & GESI, K. (1978). *J. Phys. Soc. Jpn*, **45**, 711–712.
ISHIBASHI, Y. & TAKAGI, Y. (1975). *J. Phys. Soc. Jpn*, **38**, 1715–1719.
IVANOV, I. R., KHUSRAVOV, D., SHUVALOV, L. A. & SHCHANGINA, N. M. (1979). *Izv. Akad. Nauk SSSR Ser. Fiz.* **43**, 1691–1701.
IWATA, Y., KOYANO, N. & SHIBUYA, I. (1989). *Annu. Rep. Res. React. Inst. Kyoto Univ.* **22**, 87–91.
IWATA, Y., MITANI, S., FUKUI, S. & SHIBUYA, I. (1989). *Annu. Rep. Res. React. Inst. Kyoto Univ.* **22**, 14–26.
JOHNSON, C. K. (1971). *ORTEPII.* Report ORNL-3794, revised. Oak Ridge National Laboratory, Tennessee, USA.
JONA, F. & PEPINSKY, R. (1953). *Phys. Rev.* **92**, 1577.
JONA, F. & SHIRANE, G. (1962). *Ferroelectric Crystals.* Oxford: Pergamon.
KORALEWSKI, M. (1991). Private communication.
KORALEWSKI, M. & SZAFRAŃSKI, M. (1988). *Ferroelectrics*, **80**, 269–272.
KURODA, R. & MASON, F. (1981). *J. Chem. Soc. Dalton Trans.* pp. 1268–1273.
LATUSH, L. T., RABKIN, L. M., TORGASHEV, V. I., YUZYUK, Y. I., SHUVALOV, L. A. & SHAGINA, N. M. (1987). *Ferroelectrics*, **75**, 455–468.
LOWRY, T. M. (1964). *Optical Rotatory Power.* New York: Dover.
NARDELLI, M. (1983). *Comput. Chem.* **7**, 95–98.
ROMANYUK, N. A., GABA, V. M. & KOSTETSKII, A. M. (1981). *Ukr. Fiz. Zh.* **26**, 304–308.
SANNIKOV, D. Z. & LEVANYUK, A. P. (1977). *Solid State Phys.* **19**, 118–120.
SAWADA, A. & TAKAGI, Y. (1971). *J. Phys. Soc. Jpn*, **31**, 952.

SAWADA, A. & TAKAGI, Y. (1972). *J. Phys. Soc. Jpn*, **33**, 1071–1075.

SHELDRICK, G. M. (1976). *SHELX76. Program for Crystal Structure Determination*. Univ. of Cambridge, England.

SHKURATOVA, I. G., KIOSSE, G. A. & MALINOVSKII, T. I. (1979). *Izv. Akad. Nauk SSSR Ser. Fiz.* **43**, 1685–1690.

STADNICKA, K. & BROŻEK, Z. (1991). *Acta Cryst.* B47, 484–492.

TAKAGI, Y. & MAKITA, Y. (1958). *J. Phys. Soc. Jpn*, **13**, 272–277.

Structure of the β-Blocker/Vasodilator Agent Prizidilol, DL-6-{2-[3-(*tert*-Butylamino)-2-hydroxypropoxy]phenyl}-3-pyridazinylhydrazine Hemisulfate Monohydrate

BY KEITH PROUT AND KEITH BURNS

Chemical Crystallography Laboratory, Oxford University, 9 Parks Road, Oxford OX1 3PD, England

AND ANTHONY M. ROE

*Smith Kline and French Research Ltd, The Frythe, Welwyn, Hertfordshire AL6 9AR, England*

Abstract

Prizidilol, a compound combining vasodilator and β-blocker functionalities in the same molecule, has been synthesized and characterized by Smith Kline and French Research Ltd. Crystal data: $C_{17}H_{25}N_5O_2.\frac{1}{2}H_2SO_4.H_2O$, $M_r = 398.47$, orthorhombic, $a = 10.722$ (2), $b = 11.635$ (6), $c = 34.105$ (3) Å, $V = 4254.61$ Å^3, *Pbnm* (non-standard form of *Pnma*) (D_{2h}^{16}, No. 62), $Z = 8$, $F(000) = 1704$, $D_x = 1.244$ Mg m^{-3}, μ(Cu $K\alpha$) = 11.673 cm^{-1}, $R = 0.064$ for 2432 independent reflections with $I > 3\sigma(I)$. Prizidilol shows strong conformational similarities to propranolol and is protonated at the secondary amine. The 6-phenyl-3-hydrazinopyridazine residue is not planar. The hydroxy group at the asymmetric carbon is disordered so that both enantiomers are found at each molecular site. The sulfate ions and disordered water molecules lie in the crystallographic mirror plane.

Introduction

Peripheral vasodilator agents are in clinical use to lower blood pressure: however, the reduction of blood pressure initiates the activation of β-adrenoceptors in the heart with a consequent undesirable increase in heart rate. These undesirable effects of vasodilators are inhibited by β-adrenoceptor antagonists with the result that the combined use of vasodilators and β-blockers has been widely adopted for the treatment of hypertension. An effort by Smith Kline and French Research Ltd to combine the vasodilator and β-blocker function in the one mol-

ecule led to the development of the hydrazinopyridazine, prizidilol (1) (Taylor, Cameron, Eden, Fielden & Owen, 1981; Taylor, Roe & Slater, 1979).

(1)

(2)
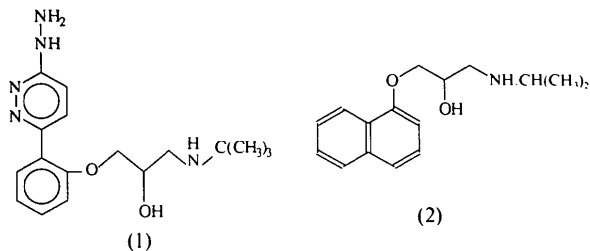
Although long-term toxicological effects prevented the completion of the development of prizidilol, substantial favourable clinical data established the therapeutic significance of the combination of vasodilator and β-blocker functions in the same molecule (Eggertsen, Andren & Hansson, 1983; Karlberg *et al.*, 1983). Here we present structural data with particular examination of the conformation of the vasodilator moiety and its β-blocker side chain.

Experimental

The needle-shaped orange crystal used for data collection (size 0.1 × 0.1 × 1.0 mm mounted on a CAD-4 diffractometer, Cu $K\alpha$ radiation) was obtained as the hemisulfate from dilute aqueous sulfuric acid solution. The unit-cell dimensions and orientation matrix were obtained from 25 carefully centred reflexions $27 < \theta < 36°$. The intensity data were collected by $\omega/2\theta$ scan, scan aperture 4 mm, graphite-monochromated Cu $K\alpha$ radiation. 4064